

UCRL 94738
PREPRINT

ELECTRICAL RESISTIVITY RESPONSE DUE TO
ELASTIC-PLASTIC DEFORMATIONS

R. B. Stout

This paper was prepared for submittal to the
ASME Symposium on Stress Measurements for Shock
Wave Applications, Cincinnati, Ohio, June 14-18,
1987.

January, 1987

Lawrence
Livermore
National
Laboratory

This is a preprint of a paper intended for publication in a journal or proceedings. Since changes may be made before publication, this preprint is made available with the understanding that it will not be cited or reproduced without the permission of the author.

DISTRIBUTION OF THIS DOCUMENT IS UNLIMITED

ELECTRICAL RESISTIVITY RESPONSE DUE TO
ELASTIC-PLASTIC DEFORMATIONS

R. B. Stout

	<u>Page</u>
Abstract.....	1
I. Introduction.....	2
II. Deformation Dependent Resistivity Response Model.....	4
III. Inference of Stress From Resistivity Changes.....	24
IV. Summary.....	36
Acknowledgments.....	38
References.....	39
Figures.....	42

DISCLAIMER

This report was prepared as an account of work sponsored by an agency of the United States Government. Neither the United States Government nor any agency thereof, nor any of their employees, makes any warranty, express or implied, or assumes any legal liability or responsibility for the accuracy, completeness, or usefulness of any information, apparatus, product, or process disclosed, or represents that its use would not infringe privately owned rights. Reference herein to any specific commercial product, process, or service by trade name, trademark, manufacturer, or otherwise does not necessarily constitute or imply its endorsement, recommendation, or favoring by the United States Government or any agency thereof. The views and opinions of authors expressed herein do not necessarily state or reflect those of the United States Government or any agency thereof.

MASTER
JHP

Electrical Resistivity Response Due to Elastic-Plastic Deformations*

R. B. Stout
Lawrence Livermore National Laboratory
P O Box 808, L-200
Livermore, CA 94550

Abstract

The electrical resistivity of many materials is sensitive to changes in the electronic band configurations surrounding the atoms, changes in the electron-phonon interaction cross-sections, and changes in the density of intrinsic defect structures. These changes are most directly dependent on interatomic measures of relative deformation. For this reason, a model for resistivity response is developed in terms of interatomic measures of relative deformation. The relative deformation consists of two terms, a continuous function to describe the recoverable displacement between two atoms in the atomic lattice structure and a functional to describe the nonrecoverable displacement between two atoms as a result of interatomic discontinuities from dislocation kinetics. This model for resistivity extends the classical piezoresistance representation and relates electric resistance change directly to physical mechanisms. An analysis for the resistivity change of a thin foil ideally embedded in a material that undergoes elastic-plastic deformation is presented. For the case of elastic deformations, stress information in the material surrounding the thin foil is inferred for the cases of pure strain coupling boundary conditions, pure stress coupling boundary conditions, and a combination of stress-strain coupling boundary conditions.

*Work performed under the auspices of the U.S. Department of Energy by the Lawrence Livermore National Laboratory under contract number W-7405-ENG-48.

I. Introduction

In many high-strain rate applications that involve shock loading it is important to perform measurements that can be used to infer the local state of stress. Such measurements support physical intuitions and provide checks on predictive analysis, whether numerical or analytical, of the stress state. However, equally important, is the use of stress measurements to understand and to correctly model the deformation response of various materials. Since stress is a symmetric second order tensor, it is not a trivial task to design a gage that measures the six independent components of stress. In fact, a gage that measures stress directly and is uncoupled from other effects is not believed possible. For example, to sense a stress change involves an instrument that actually measures or has a coupling with a deformation response.

The particular case of interest here is the use of piezoresistive materials in stress gage design. There are several metallic and organic materials that have a significant electrical resistance change that has been correlated with pressure, hence, the name piezoresistivity [1-4]. However, the intrinsic physical mechanisms responsible for the electrical resistivity are more directly dependent on various deformation measures and the density of various defect structures rather than the stress tensor [4-11]. Thus, it is logical to initially represent the electrical resistivity response of a material in terms of deformation dependent functions and defect structure dependent functions. This is the approach that is taken in Section II, where the deformation includes both recoverable (elastic) and nonrecoverable (plastic) deformations. The nonrecoverable deformation depends on the defect structure, which for the analysis of Section II is limited to dislocation density effects. This dislocation dependence restricts the generality of the model to essentially metallic piezoresistance materials such as ytterbium and manganin. Consequently, nonrecoverable deformations from microcrack density effects, which are a more probable dependence in the resistivity response of organic materials, is not represented.

There have been several models and discussions of elastic piezoresistivity [1,2,12-18]. The elastic-resistivity models follow the approach of Bridgeman's early work [12], and take a phenomenological viewpoint of representing the observed resistivity change as a function of stress. Much of the laboratory experimental effort has been directed toward understanding, applying, and calibrating the piezoresistivity response for purposes of measuring stress during shock loading [14-29]. The field applications of the piezoresistance response are for stress measurements from chemical and/or nuclear explosives [30-37]. In addition to the elastic-resistivity response, observations of resistivity changes during plastic deformations [17,23] showed a permanent, or nonrecoverable, change in resistivity. It is important to understand the origin and the representation of these nonrecoverable or permanent changes in resistivity for applications involving the measurement of residual stress states [34]. Thus, a change in gage resistivity after a shock experiment is completed could result from a residual stress state on the gage and/or a nonrecoverable deformation of the piezoresistance material in the gage.

This nonrecoverable resistivity, as well as the recoverable resistivity, has been recently studied in greater detail by Chen, Gupta, and Miles [23]. In this work, the resistivity response of three difficult materials, manganin, ytterbium, and constantan, were experimentally studied for quasi-static, elastic-plastic, uniaxial strain histories. In addition to the experiments, a phenomenological model for the elastic-plastic resistivity response of these three materials was proposed. The model represented the change in resistivity as a function expressed in terms of stress variables and plastic strain variables. As developed, this model [23] is rate-independent. Furthermore, the hysteresis resistivity response that was observed during unloading and reloading from a plastic strain was not represented by this model. The type of resistance hysteresis illustrated by the experimental data suggests that the dislocation density around Frank-Read sources is changing during unloading. If this were the case, then the resistivity response is probably strain-rate dependent. Furthermore, the resistivity hysteresis loop during initial unloading has a slope that is different from the initial elastic loading resistivity slope and from the initial reloading resistivity slope. Thus, for purposes of understanding and interpreting residual stress, there is a need to extend the elastic-plastic resistivity model of Chen, Gupta, and

Miles [23]. An extension is developed in Section II where the physical mechanisms of electron resistivity are discussed relative to stress gage design.

In Section III, the problem of relating a measured resistivity change to a stress state on a gage is discussed and shown not to be necessarily unique. In general, and if possible, the gage must be designed to uniquely isolate or separate the stress tensor components that are of interest and are to be measured. Otherwise, the resistance measurement from a single gage of a particular material is coupled to all components of the stress or strain tensor through the elastic-resistivity tensor of the material and the geometrical size changes of the gage. For the special case of resistivity changes due only to the three independent diagonal elements of the strain tensor, or the stress tensor for the elastic case (no shear resistivity dependence), it is conceptually possible to measure the resistivity response from three different materials and have three independent and simultaneous measurements. Then, if the resistivity tensor of each material is independent of the other materials, a unique inverse for the three diagonal components of the strain or stress tensor can be performed. For the case of a gage embedded in a material, the boundary conditions between the gage and the surrounding material determine the deformation response of gage. For a gage bonded to the surrounding material, and ignoring shear in the thin gages, the gage would sense the stress component normal to the plane of the gage and the strain components tangent to the plane of the gage. This requires a mixed analysis of components in the stress and strain tensors to infer the resistivity response of a gage. The strain, stress, and mixed stress-strain conditions are discussed in greater detail in Section III. This discussion provides a possible resolution to some of the problems of inferring stress response from resistivity measurements.

II. Deformation Dependent Resistivity Response Model

The electrical resistivity of a material is a measure related to the number and velocity of electrons flowing through the material's atomic arrangement. With respect to a deformation dependence, some sensitive intrinsic mechanisms of resistivity are the electronic band configurations of

the atomic arrangement, the electron-phonon interaction cross sections, and the density of defect structures in the atomic arrangements [3-8]. The type of electronic band configuration determines primarily the available number of mobile electrons. The electron-phonon interaction and the density of defect structures determine primarily the number and degree of scattering events that impede the transport of electrons, and thereby, change the velocity of the mobile electrons.

A starting point for a physical model of deformation-dependent resistivity of a material is the definition of electric current, which is an electron flux, namely,

$$\underline{J}_i = \int_{\{V\}} e N^* \underline{v}_i dV \quad (2-1)$$

where \underline{J}_i is the electric current vector, e is the charge per electron, N^* is a functional and represents the probabilistic number density of electrons distributed over the velocity vector \underline{v} of the electrons, and $\{V\}$ is the domain of possible electron velocities. In order to correctly represent the physical recoverable and nonrecoverable deformation dependence of resistivity, the electron flux vector \underline{J} will be first defined per an individual atom of the material. Thus, the electron density is also defined in terms of the number of electrons per atom. This is initially cumbersome; however, the usual electron flux measure of charge per unit area per unit time for a non-deforming resistor can be easily obtained by using the atomic number density per unit volume of the material. The time-dependence of the atomic number density during a deformation process is described by a conservation principle that is analogous to the conservation of mass. This particular definition for current is used to provide a clear physical representation of the recoverable and nonrecoverable deformation dependence. Thus, during a recoverable deformation, which is like an elastic deformation of continuum mechanics, the atomic arrangement of the material is described by a continuous function. Hence, the number of atoms in a lattice plane remains constant as the lattice plane undergoes the deformation process. However, during a nonrecoverable deformation process that involves dislocations, the number of atoms in a lattice plane need not remain constant. This merely means that a thin foil of a material being stretched uniaxially can have a permanent change in thickness from dislocations gliding across lattice planes. The amount of

this nonrecoverable thickness change depends on the species of the dislocation, but essentially the cross-sectional area of the foil is locally reduced by an atom spacing per dislocation glide. In terms of the previous definition for elastic current per atom, an integration for the total current of the reduced cross section would sum over fewer atoms after the dislocation glide. Hence, the nonrecoverable deformation dependence of resistance response requires that special attention be given to the initial definition of electric current. Certainly, the later development of the nonrecoverable deformation dependence will be more direct and easier to understand because of this definition.

At this point, a deformation-dependent resistivity model has to be discussed in terms of the deformation process, and how the kinematics of the deformation process change the terms in the integrand of equation (2-1). The first term is the charge per electron, which is not changed by the limited deformations considered here. The next term is the number density of electrons. From various discussions of electronic band theory [3-8], particularly for the transition metals that have unfilled intermediate electronic shells and overlapping conduction bands, the relative deformation between adjacent atoms can cause a change in the available density of mobile electrons. Thus, the number density N^* should depend on some deformation measure involving changes in the relative interatomic spacing. Furthermore, the density of defect structures [6-11], which for purposes here is described in terms of dislocation density, can have an influence over the associated number of mobile electrons per atom. This is because the core of a dislocation disrupts the regular atomic spacing of a crystalline lattice structure; hence, the electronic band configuration in the neighborhood of a dislocation core may be perturbed and cause a local density change in the available number of mobile electrons.

Finally, the last term of the integrand is the velocity of the electron density functional; in terms of a statistical mechanics formulation [6,7] for electron transport this velocity is more like a coordinate parameter rather than a function. However, for current to flow, the electron velocity is related to the applied force of the electric field. The electron velocity relationship to the electric field can be developed either by a statistical formulation that would use a Boltzmann's equation or by evaluating the average electron velocity for the given electron density function by formally

integrating over the domain $\{V\}$. From a formal integration of equation (2-1) over $\{V\}$, an average electron velocity expression is defined by

$$\underline{J} = N \bar{\underline{V}} \quad (2-2)$$

where the average velocity $\bar{\underline{V}}$ of all the electrons is defined by the integration process and the functional N for electron charge density no longer depends on the velocity parameter, but only on deformation measures and the defect density. The average velocity of electron flow is related to the applied electric field vector [3-5], which can be represented as

$$\bar{V}_i = c_{ij} E_j \quad (2-3)$$

where E_j is the applied electric field vector and c_{ij} is a second order tensor to relate the electric field to the average electron velocity. Thus, c_{ij} is an electron transport conductive tensor. The tensor c_{ij} is also a functional quantity that depends on the deformation, and possibly the electric field if nonlinear electrical effects are to be modelled. Some deformation dependence in the tensor c_{ij} is expected because changes in the interatomic spacing can cause the electron-phonon scattering cross sections to change. Also, deformation processes that change the dislocation density function change the number of lattice defect sites that scatter and impede the velocity of the electrons.

In order to represent deformation-dependent expressions for the two functionals of electron density N and the electron transport conductive tensor c_{ij} , some background into relative deformations between atoms must be presented. The following review considers both recoverable and nonrecoverable deformations; and the nonrecoverable part will be dependent only on dislocation kinetics [38-40]. The relative deformation between any two atoms, say atom A and atom B, can be separated into a recoverable term and a nonrecoverable term. The recoverable term represents the continuum deformation of the atomic lattice; hence, it can be represented by a continuous function. The nonrecoverable terms represent primarily the discontinuum deformation as neighboring atoms are repositioned by an amount equal to the Burgers' vector of dislocations that move between the atomic lattice planes. This nonrecoverable term is also a functional that represents the accepted physical mechanism of discontinuous motion and displacement between atoms from dislocations transported

through the atomic lattice of a material. In equation form, the relative deformation is given as

$$\underline{x}\}(A \rightarrow B, t) = \underline{x}\}(A \rightarrow B) + \underline{u}\}(A \rightarrow B, t) + \underline{u}\}(A \rightarrow B, t) \quad (2-4)$$

where

- $\underline{x}\}$ vector from atom A to atom B at time $\tau = t$,
- $\underline{x}\}$ vector from atom A to atom B at time $\tau = 0$,
- $\underline{u}\}$ recoverable lattice displacement of atom B relative to atom A at time $\tau = t$,
- $\underline{u}\}$ nonrecoverable displacement of atom B relative to atom A, during the time interval $[0, t]$ due to dislocation kinetics.

In words, equation (2-4) is a statement that the relative deformation vector $\underline{x}\}$ between two atoms A and B at time $\tau = t$ is given by the initial value $\underline{x}\}$ plus a recoverable displacement $\underline{u}\}$ plus a nonrecoverable displacement $\underline{u}\}$. This is illustrated in Figure 2-1, which shows an undeformed lattice structure at time $\tau = 0$ and a deformed lattice structure at time $\tau = t$. Note from the figure that the initial left to right number of lattice spacings between atoms B and A is one; however, at $\tau = t$ the number of left to right lattice spacings between atoms B and A has increased to five. Thus, not only have the lattice planes been deformed, which is the recoverable deformation, but also dislocations have glided between atoms B and A to discontinuously displace some of the lattice planes relative to each other.

As mentioned previously, and discussed elsewhere [39,40], the mathematical representation of the recoverable displacement is that of continuous functions to describe the shape of the lattice structure. The mathematical representation for the nonrecoverable part is a functional that depends on the dislocation density function. The dislocation density of this discontinuum formulation is a statistical measure for the probable number of dislocations per species per unit volume. For crystalline solids a particular species of dislocations is identified by a Burgers' vector \underline{b} , a vector $\underline{\xi}$ that is tangent to the line of the dislocation, and a velocity vector \underline{v} that is the velocity of the dislocation relative to the local lattice structure. This dislocation density function is denoted by $D(\underline{x}, t, \underline{b}, \underline{\xi}, \underline{v}) d\underline{b} d\underline{\xi} d\underline{v}$, which is the probable number of dislocation

species $(\underline{b}, \underline{\xi}, \underline{v})$ in a species volume $d\underline{b}d\underline{\xi}d\underline{v}$ per unit spatial volume about point \underline{x} at time t . For shorthand notational purposes, a dislocation species $(\underline{b}, \underline{\xi}, \underline{v})$ will be denoted by \underline{g} , and the domain of all species will be denoted by Q . Using this density function, the non-recoverable displacement of atom B relative to atom A can be represented with two terms such that one term depends on dislocation motion and the other term depends on dislocation density changes. The expression is given by

$$u_{ij}(A \rightarrow B, t) = \int_0^t \int_{\underline{x}(A, \tau)}^{\underline{x}(B, t)} \int_Q (b_i e_{jkl} \xi_k v_l D(\underline{x}, t, \underline{g})) + b_i e_{jkl} \xi_k b_l^* (\partial_\tau f(\underline{x}, t, \underline{g}) + \partial_m (\bar{v}_m D(\underline{x}, t, \underline{g}))) d\underline{g} dx_j(A \rightarrow B, \tau) d\tau \quad (2-5)$$

From dislocation theory, the first term $b_i e_{jkl} \xi_k v_l$ of the above integrand is the relative displacement of an atom on one lattice plane with respect to an atom on an adjacent lattice plane as a single dislocation moves between the two lattice planes and sweeps out an area rate that is given by the vector cross-product of the line tangent ξ_k and the velocity v_l ; $e_{jkl} \xi_k v_l$. By multiplying the first term by the dislocation density $D(\underline{x}, \tau, \underline{g})$, and first integrating over all species \underline{g} in Q , next integrating over every lattice plane between atom A and B, and finally, integrating over the time interval $(0, t)$, the net discontinuity u_{ij} from dislocation motion is determined. This discontinuous displacement is usually dislocation glide motion, but can also include dislocation climb. In dislocation theory, pure glide motion does not result in a local volume change. However, dislocation climb or dislocations that intersect and cut through the lines of other dislocations can result in a local volume change because these processes are inter-related with vacancy and interstitial lattice kinetics. The second term of the integrand represents the relative displacement between atoms A and B due to dislocation density changes along the line of integration $dx_j(A \rightarrow B, \tau)$. The measure of the displacement is from the term $b_i e_{jkl} \xi_k b_l^*$; where the vector b_l^* accounts for the magnitude and direction of the relative displacement when a change in the dislocation density occurs. For example, if an edge dislocation were created between two adjacent atoms, then this dislocation density change results in a relative

displacement given by the Burgers' vector b_i . Again, one performs the integration for the contribution to displacement from dislocation density changes over all dislocation species g in species space Q , then an integration over each lattice plane between the positions of atoms A and B at time τ along the line segments $dx_j(A \rightarrow B, \tau)$, and finally an integration over all times τ in the interval $(0, t)$.

Equation (2-4) represents the relative deformation between two arbitrary atoms A and B. From the previous discussion of electronic band configurations, it is the relative deformation between atoms that would be a physically appropriate deformation measure to express changes in the electronic band configurations. Furthermore, the relative deformation between atoms would be appropriate to represent changes in the electron-phonon interaction cross sections. In both of these cases, one can visualize the relative motion of neighboring atoms changing both the electronic energy levels, as the electronic bands overlap, and the phonon spectrum along with the associated interaction cross sections, as the atoms move closer or farther apart. It is not, however, as easy to visualize all the physical effects from dislocation kinetics and to see how the physical effects should be best represented.

There are, however, some resistivity changes that depend on reasonably well understood dislocation kinetics. The two physical effects that readily suggest dislocation dependent deformation measures are the defect cross section for electron-dislocation scattering [6-10] and the cross-sectional area and length changes of the material body as a result of nonrecoverable deformation from dislocation glide. A direct dislocation density dependence for electron scattering has been modelled by Brown [9,10], and the scattering depends on the cross-section of the dislocation core. The cross-sectional area and length change of the material can be calculated for rectangular shape foils commonly used in piezoresistance stress gages for cases of homogeneous or spatial uniform dislocation kinetics.

The physical effects from dislocation kinetics that are not well understood involve the electronic band configurations. For example, the physical effect or relationship between dislocation density and the electronic band configurations, and any subsequent interatomic deformations, is not presently well-known. However, it is reasonable to assume that such an effect exists because the core volume around a dislocation line separates neighboring

atoms and disrupts the normal electronic band configuration of the regular crystalline lattice structure. Furthermore, the core volume of a dislocation line results in a localized strain field in the crystalline lattice structure near the dislocation. Based on this discussion, the core volume of the dislocation density would be a deformation measure to use as a function dependence in both electronic band configuration and localized strain field effects during dislocation kinetics. In fact, a measure of dislocation core volume per unit volume would be somewhat like a volume strain measure. Such a measure can be readily defined in terms of the dislocation species parameters and the dislocation density function. For example, the core volume for a particular dislocation species is simply the inner vector product of the cross-sectional area vector of the core, which depends on the particular species $(\underline{b}, \underline{\xi}, \nu)$, and the tangent vector $\underline{\xi}$ of the dislocation.

The above discussion provides sufficient physical background to represent resistivity response in terms of deformation dependent measures. First, consider the electron density functional N of equation (2-2); clearly, N would certainly depend on a deformation measure that describes the changes in atomic separation and on a deformation measure that describes lattice changes from dislocation kinetics. Changes in atomic separation are measured by the relative deformation $\underline{\chi}$ of equation (2-4), however, for a simple model of electron density changes that involves only nearest atomic neighbors surrounding an arbitrary atom and small deformations, a dependence on $\underline{\chi}$ can be approximated by a dependence on the local recoverable strain tensor and an approximation for the nonrecoverable strain tensor. This approximation follows from equations (2-4) and (2-5) by letting atom B approach a nearest neighbor position of atom A and using a small deformation approximation to replace the integration limits $\underline{\chi}(A, \tau)$ and $\underline{\chi}(B, \tau)$ with $\underline{\chi}(A, 0)$ and $\underline{\chi}(B, 0)$ in equation (2-5). This gives a continuum result for the recoverable lattice strain tensor and a discontinuum approximate result for the nonrecoverable strain tensor due to dislocation kinetics. These two strain tensors define a total strain tensor in the neighborhood of atom A to atom B given by

$$\underline{\chi}_A^j = \underline{\chi}_A^j{}^B + \underline{\chi}_A^j{}^B \quad (2-6)$$

where $\underline{\gamma}_A^B$ is the total strain tensor and the recoverable lattice tensor $\underline{\gamma}_l$ is

$$\underline{\gamma}_l = \Delta \gamma_{ji}^l = 1/2(\Delta_j u_i^l + \Delta_i u_j^l + \Delta_j u_k^l \Delta_i u_k^l) \quad (2-7)$$

and the nonrecoverable strain tensor $\underline{\gamma}$ is approximated for small deformations by

$$\begin{aligned} \underline{\gamma} = \gamma_{ji} = 1/2 (\Delta_j u_i + \Delta_i u_j + \Delta_j u_k \Delta_i u_k \\ + \Delta_j u_k \Delta_i u_k + \Delta_j u_k \Delta_i u_k) \end{aligned} \quad (2-8)$$

which couples the recoverable and nonrecoverable displacements. In the above expressions, the $\underline{\Delta}()$ operator is used to denote a partial derivative relative to the atomic lattice spacing size, and replaces the usual point-wise partial derivative notation of continuous function theory. For the lattice strain tensor $\underline{\gamma}_l$, the $\underline{\Delta}()$ operator is retained even though the lattice displacement u^l is assumed to be a continuous function. The $\underline{\Delta}()$ operator on the dislocation dependent relative displacement is approximated by

$$\Delta_j u_k = \int_0^t \int_Q (b_i e_{jkl} \dot{\xi}_k v_l D + b_i e_{jkl} \dot{\xi}_k b_l^* \dot{D}) \, dq \, dt \quad (2-9)$$

which is an expression very similar to equation (2-5) except that the spatial integration has been removed by using the small deformation approximation, and the rate of dislocation density change is defined by

$$\dot{D}(\underline{x}, \tau, Q) \equiv \partial_t D + \partial_m (\dot{v}_m D) \quad (2-10)$$

Additional dislocation dependent operators $\underline{\hat{\Delta}}$ and $\underline{\Lambda}$ are defined for purposes of shorter notation as

$$\underline{\hat{\Delta}}() = \hat{\Delta}_{ij}() \equiv \int_Q b_i e_{jkl} \dot{\xi}_k v_l() \, dq \quad (2-11a)$$

$$\underline{\Lambda}() = \Lambda_{ij}() \equiv \int_Q b_i e_{jkl} \dot{\xi}_k b_l^*() \, dq \quad (2-11b)$$

With the above definitions of operators, equation (2-9) becomes

$$\underline{A}_{ij} u_i] = \int_0^t \underline{A}_{ij} \dot{D} + \underline{A}_{ij} \dot{\underline{D}} \, dt \quad (2-12a)$$

or equivalently in vector notation

$$\underline{A} \underline{u}] = \int_0^t \underline{A} \dot{D} + \underline{A} \dot{\underline{D}} \, dt \quad (2-12b)$$

Using the above strain measures, a functional involving the total relative deformation can be expanded, for small deformations, in terms of the recoverable and nonrecoverable strain tensors; providing that the intrinsic lattice rotation effects are not important. Thus, for any smooth functional f with respect to the argument $\underline{x}]$, an approximate expansion up to first order terms in local relative displacements and then strains is

$$f(\underline{x}]) \doteq f(\underline{X}] + \underline{A}_{u}] f(\underline{X}] \underline{u}] + \underline{A}_{\gamma}] f(\underline{X}] \underline{\gamma}] \quad (2-13a)$$

$$\doteq f(\underline{X}] + \underline{A}_{\underline{u}]} f(\underline{X}] \underline{u}] + \underline{A}_{\underline{\gamma}]} f(\underline{X}] \underline{\gamma}] \quad (2-13b)$$

where $\underline{A}_{u}] f$, $\underline{A}_{\underline{u}]} f$, $\underline{A}_{\underline{\gamma}]} f$, and $\underline{A}_{\underline{\gamma}]} f$ are functional operators of the functional f for variations in the recoverable lattice displacement $\underline{u}]$, the nonrecoverable displacement $\underline{u}]$, the recoverable lattice strain tensor $\underline{\gamma}]$, and the nonrecoverable strain tensor $\underline{\gamma}]$, respectively; and $f(\underline{X}]$ is the value of the functional at zero displacements and/or strains. It is this type of representation that will be used to express a relative deformation dependence for the electron density functional N . But first, an explicit measure of deformation related to dislocation core volume is required to complete the functional representation of N on dislocation density.

As discussed earlier, a measure of dislocation core volume is the cross sectional area of a dislocation core times the length of the associated dislocation. Here, it will be assumed that the cross-sectional area of a dislocation core can be described in terms of the species attributes $\{b, \xi, v\}$. Then, denoting this area as vector $\underline{\phi}$ whose direction is tangent to the dislocation line, the volume of a dislocation segment of length ξ is

$$\alpha^* = \phi_k \xi_k = \Phi \cdot \Xi \quad (2-14)$$

To find the volume due to a given density of dislocation D_0 , consider α^* as an operator per unit species; then the dislocation volume measure per unit volume is given by

$$\alpha_0 = \int_Q \phi_k \xi_k D_0 \, dq \quad (2-15)$$

For notational purpose, an operator $\Delta_D \alpha$ over all species and times up to t is defined as

$$\Delta_D \alpha(\cdot) \equiv \int_0^t \int_Q \phi_k \xi_k(\cdot) \, dq \, dt \quad (2-16)$$

This operator is defined to relate electron density changes to dislocation kinetics because it is the change in dislocation density that is relevant. Thus, at any time t greater than 0 after a given initial density D_0 , the dislocation volume per unit volume denoted by $\alpha(\underline{x}, t)$ is

$$\alpha(\underline{x}, t) = \alpha_0(\underline{x}) + \Delta_D \alpha(\underline{x}, \tau, q) \quad (2-17)$$

where α_0 is defined in equation (2-15) and the $\Delta_D \alpha$ operator of equation (2-16) includes integrations over time and species to represent the change in dislocation core volume from dislocation kinetics.

Using the strain tensors and the dislocation core volume as arguments of the electron density functional N , a first order expansion about zero strain and an initial α_0 core volume is analogous to equation (2-13), namely,

$$N(\underline{x}, t; \underline{\gamma}_I, \underline{\gamma}_J, \alpha) = N_0(\underline{x}, t; \alpha_0) + \underline{\Delta}_{\underline{\gamma}_I} N \underline{\gamma}_I + \underline{\Delta}_{\underline{\gamma}_J} N \underline{\gamma}_J + \underline{\Delta}_{\alpha} N \Delta_D \alpha \quad (2-18)$$

where $\underline{\Delta}_{\underline{\gamma}_I} N$, $\underline{\Delta}_{\underline{\gamma}_J} N$, and $\underline{\Delta}_{\alpha} N$ can be, in general, dependent on the arguments $\underline{\gamma}_I$, $\underline{\gamma}_J$ and α ; but in a simple model would be given by two second order tensors and a scalar, respectively. The representation for electron density per atom

given in equation (2-18) provides for the initial electron density N_0 , plus a change from recoverable strains given by $\Delta_{\underline{\gamma}} N \underline{\gamma}$, plus a change from non-recoverable strains given by $\Delta_{\underline{\gamma}} N \underline{\gamma}$, and finally a change from core volume of new dislocations given by $\Delta_{\alpha} N \Delta_D \alpha \bar{D}$. For material samples that are comprised primarily of one element, almost all atomic neighborhoods remain the same atom species before and after the nonrecoverable interatomic displacements. Thus, the coefficient $\Delta_{\underline{\gamma}} N$ would probably be small and nonrecoverable strain effects that depend on the functional N defined per atom would be insignificant in this case. This intrinsic or local effect of nonrecoverable strain on resistivity change is clearly separate and distinct from a global effect of nonrecoverable strains that results from permanent dimensional changes of the material specimen. The permanent dimensional changes will be modelled after the intrinsic representation for the electron transport conductive tensor c_{ij} of equation (2-3) is completed.

The functional c_{ij} depends on interatomic relative deformations and dislocation density, which influence the electron-phonon and electron-defect scattering cross sections. Thus, analogous to equation (2-18), the deformation measures to represent those physical effects will be taken as the strain tensors and the dislocation core volume. Then, a first order expansion about zero strain and the initial α_0 core volume is given for the tensor functional \underline{c} by

$$\underline{c}(\underline{x}, t; \underline{\gamma}, \underline{\gamma}, \alpha) = \underline{c}_0(\underline{x}, t; \alpha_0) + \Delta_{\underline{\gamma}} \underline{c} \underline{\gamma} \quad (2-19)$$

$$+ \Delta_{\underline{\gamma}} \underline{c} \underline{\gamma} + \Delta_{\alpha} \underline{c} \Delta_D \alpha \bar{D}$$

where $\Delta_{\underline{\gamma}} \underline{c}$, $\Delta_{\underline{\gamma}} \underline{c}$, and $\Delta_{\alpha} \underline{c}$ can be, in general, dependent on the arguments $\underline{\gamma}$, $\underline{\gamma}$, and α ; but in a simple model would be given by two fourth order tensors and a second order tensor operator, respectively. The representation for electron transport impedance given by equation (2-19) provides for an initial impedance to electron mobility given by the tensor \underline{c}_0 , plus a change from recoverable strains given by $\Delta_{\underline{\gamma}} \underline{c} \underline{\gamma}$, plus a change from nonrecoverable strains given by $\Delta_{\underline{\gamma}} \underline{c} \underline{\gamma}$, and finally a change from core volume of new dislocation given by $\Delta_{\alpha} \underline{c} \Delta_D \alpha \bar{D}$. The effect of nonrecoverable strains on electron

transport conductance are expected to be small for a material sample comprised primarily of atoms from one element; thus, the coefficient $\frac{\Delta_{\gamma}}{\underline{c}}$ is also expected to be small in this case.

This completes the representations for the two independent terms in the integrand of equation (2-2). The two representations of equations (2-18) and (2-19) are now substituted into equation (2-2) to give the following expression;

$$\begin{aligned} \underline{J} = & (N_0 + \frac{\Delta_{\gamma}}{\underline{c}} N_{\gamma} | + \frac{\Delta_{\gamma}}{\underline{c}} N_{\gamma}] + \Delta_{\alpha} N_0 \alpha \dot{\bar{D}}) (\underline{c}_{\underline{c}0} + \frac{\Delta_{\gamma}}{\underline{c}} \underline{c} | \underline{c} | \\ & + \frac{\Delta_{\gamma}}{\underline{c}} \underline{c} | \underline{c} |] + \Delta_{\alpha} \underline{c} \Delta_D \alpha \dot{\bar{D}}) \underline{c} \end{aligned} \quad (2-20)$$

The terms of equations (2-20) can be multiplied together to give the following expression for intrinsic current per atom;

$$\begin{aligned} \underline{J} = & (\underline{r}_{\underline{c}0} + \underline{r}_{\gamma} | \underline{c} | + \underline{r}_{\gamma}] \underline{c} | + \underline{r}_{\underline{c}0} \dot{\bar{D}} \\ & + \underline{r}_{\gamma} | \underline{c} | \underline{c} | \underline{c} | + \underline{r}_{\gamma} | \underline{c} | \underline{c} | \underline{c} |] + \underline{r}_{\gamma}] \underline{c} | \underline{c} | \\ & + \underline{r}_{\gamma} | \underline{c} | \underline{c} | \dot{\bar{D}} + \underline{r}_{\gamma}] \underline{c} | \underline{c} | \dot{\bar{D}} + \underline{r}_{\underline{c}0} \dot{\bar{D}} \dot{\bar{D}}) \underline{c} \end{aligned} \quad (2-21)$$

where the operator coefficients in equation (2-21) are defined by the multiplications in equation (2-20) as

$$\underline{r}_{\underline{c}0} \equiv N_0 \underline{c}_{\underline{c}0} \quad (2-22a)$$

$$\underline{r}_{\gamma} | \equiv N_0 \frac{\Delta_{\gamma}}{\underline{c}} \underline{c} | \underline{c} + \underline{c}_{\underline{c}0} \frac{\Delta_{\gamma}}{\underline{c}} N \quad (2-22b)$$

$$\underline{r}_{\gamma}] \equiv N_0 \frac{\Delta_{\gamma}}{\underline{c}} \underline{c} + \underline{c}_{\underline{c}0} \frac{\Delta_{\gamma}}{\underline{c}} N \quad (2-22c)$$

$$\underline{r}_{\underline{c}0} \dot{\bar{D}} \equiv (N_0 \Delta_{\alpha} \underline{c} + \underline{c}_{\underline{c}0} \Delta_{\alpha} N) \Delta_D \alpha \quad (2-22d)$$

$$\underline{r}_{\gamma} | \underline{c} | \equiv \frac{\Delta_{\gamma}}{\underline{c}} | N \frac{\Delta_{\gamma}}{\underline{c}} | \underline{c} \quad (2-22e)$$

$$\underline{r}_{\gamma} | \underline{c}] \equiv \frac{\Delta_{\gamma}}{\underline{c}} | N \frac{\Delta_{\gamma}}{\underline{c}} | \underline{c} + \frac{\Delta_{\gamma}}{\underline{c}} | N \frac{\Delta_{\gamma}}{\underline{c}}] \underline{c} \quad (2-22f)$$

$$\underline{r}_{\gamma}] \underline{c} | \equiv \frac{\Delta_{\gamma}}{\underline{c}}] N \frac{\Delta_{\gamma}}{\underline{c}} | \underline{c} \quad (2-22g)$$

$$\underline{\underline{\epsilon}}_{\gamma|U} \equiv (\underline{\underline{\epsilon}}_{\gamma|N} \Delta_{\alpha\epsilon} + \Delta_{\alpha N} \underline{\underline{\epsilon}}_{\gamma|\epsilon}) \Delta_D^{\alpha} \quad (2-22h)$$

$$\underline{\underline{\epsilon}}_{\gamma|D} \equiv (\underline{\underline{\epsilon}}_{\gamma|N} \Delta_{\alpha\epsilon} + \Delta_{\alpha N} \underline{\underline{\epsilon}}_{\gamma|\epsilon}) \Delta_D^{\alpha} \quad (2-22i)$$

$$\underline{\underline{\epsilon}}_{DD} \equiv \Delta_{\alpha N} \Delta_D^{\alpha} \Delta_{\alpha\epsilon} \Delta_D^{\alpha} \quad (2-22j)$$

Equation (2-21) is a consistent approximate model if the higher order terms omitted in the first order expansions given by equations (2-18) and (2-19) are small relative to the cross-product terms and squared terms defined in equations (2-22). Even though the development of terms in equation (2-21) was based on physical concepts of electron transport and scattering terms, experimental data are required to test the adequacy of terms in equation (2-21) to represent well intrinsic resistivity response. Such data are not available since the measurement of intrinsic resistivity per atom is not experimentally performed. What is measured is the voltage response across a material specimen subjected to a prescribed stress and/or deformation history and usually under the condition of a fixed total current through the specimen [17,23]. The condition of fixed total current causes the local electric field in the test specimen to change as the resistivity changes during the prescribed stress and/or deformation history. This change of the electric field, when integrated in the direction of current flow, is the voltage across the test specimen. This voltage is measured to then infer the total resistance change for the test specimen.

In order to separate the various contributions to the total resistance change of a test specimen, equation (2-21), which is current per atom, must be integrated over the atom density of the test specimen that exists in the current state of deformation. In general, such an integration is not possible except for the simplest cases of a deformation history. Fortunately, the geometrical shapes of the material test specimens used to determine resistivity are selected to be uniform in a length direction and with a cross sectional area that is either a circular wire or else a rectangular shaped thin foil. During the experiment, the deformation response within the test specimens is taken to be spatially uniform throughout the material test specimen in either the stress or strain tensors. Of course, the time history

of the stress and strain are interdependent. However, as demonstrated by the experiments of Ginsberg et al. [17] and Chen, et al. [23], a knowledge of the current stress state is not sufficient to determine the current strain state because of the nonrecoverable contributions to the strain and deformation from dislocations. Nonetheless, the explicit assumption of a spatial uniform strain state in the material test specimen is almost required to perform a spatial integration of equation (2-21) that results in a reasonably simple and useful expression for total resistivity. For purposes here, this is placed as a restriction and is stated explicitly:

A2.1 In order to integrate the electron current equation (2-21) to define total resistivity response of a material specimen during a prescribed deformation history, the material specimen is assumed to be a thin foil and the prescribed deformation history is restricted such that only spatially uniform strain and dislocation density histories occur in the material specimen.

The assumption A2.1 corresponds to the desired experimental test conditions under which resistivity should be measured. In the case of stress gage designs that sense a resistivity change, it would also be a reasonable design constraint to require that the gage be configured in shape and geometry to have spatially uniform states of strain. This design constraint, if possible to implement, would simplify the interpretation of the resistivity measurement and improve the quality of the inference as to the strain or stress history that surrounds and loads the gage. However, if the strain and dislocation kinetics are not spatially uniform, the volume integration is very difficult.

To facilitate shorter notation during the integration, the coefficients of the electric field vector in equation (2-21) will be combined and written as a single strain and dislocation dependent tensor \underline{r} . Then equation (2-21) becomes

$$J_k = r_{kj} E_j \quad (2-23)$$

Now, equation (2-23) can be multiplied by atom density per unit volume, and for a long, thin foil of rectangular cross section, be integrated over the deformed

configuration. The integration of equation (2-23) over the deformed configuration of the material test specimen is given by

$$\int_{x_3} \int_{x_2} \int_{x_1} (J_k - r_{kj} E_j) a(\underline{x}, t) dx_1 dx_2 dx_3 = 0 \quad (2-24)$$

where the atomic number density $a(\underline{x}, t)$ is at the time t of the deformation history, the tensor r_{kj} is evaluated at the history dependent values of strain and dislocation density at time t , and the volume domain of integration for the foil test specimen is along the deformed length x_1 in the x_1 coordinate direction, the deformed width x_2 in the x_2 coordinate direction, and the deformed thickness x_3 in the x_3 coordinate direction. For this experimental geometry, only the integrated E_1 and J_1 components of electric field and electron current along the x_1 length coordinate of the foil are recorded during a resistivity measurement. Furthermore, the test specimen is taken as materially homogeneous and the deformation history of strain and dislocation density has been assumed spatially uniform. Therefore, the order of the integrations over x_1 , x_2 and x_3 coordinates can be freely interchanged and the tensor r would not depend on the spatial coordinate \underline{x} in the test specimen, but only on time t . Using the above, and the experimental condition that the total current flowing through the test specimen is a constant value throughout the history of the deformation, the current integration can be written as

$$\int_{x_1} \int_{x_2} \int_{x_3} J_1 a dx_3 dx_2 dx_1 = \frac{I_1 a}{x_2 x_3} x_1 x_2 x_3 \quad (2-25)$$

$$\equiv \frac{I_1 a^*}{x_2 x_3}$$

where I_1 is the constant electron current maintained in the deformed cross-sectional area $x_2 x_3$ during the experiment and a^* is the total number of atoms in the material test specimen because the uniform deformation history requires that the number of atoms be given by atomic density multiplied by the volume

$$a^* = a x_1 x_2 x_3. \quad (2-26)$$

The other term to be integrated in equation (2-24) is the (1-1) component of the electron impedance tensor and the electric field multiplied by the atomic density. This integration gives

$$\int_{x_1} \int_{x_2} \int_{x_3} r_{11} E_1 a \, dx_3 dx_2 dx_1 = r_{11} a \int_{x_3} \int_{x_2} \int_{x_1} E_1 dx_1 dx_2 dx_3$$

$$\equiv r_{11} a \{ \Phi_1 / x_2 \} x_3 \} \quad (2-27)$$

$$= \frac{r_{11} \Phi_1}{x_1} a^*$$

where r_{11} and a are independent of the spatial coordinate \underline{x} and the integrated electric field across the test specimen becomes the electric potential, Φ_1 , or voltage change, across the test specimen, which can be rewritten in terms of the total number of atoms and an averaged electric field quantity Φ_1/x_1 .

Combining equations (2-25) and (2-27),

$$r_{11} \Phi_1 a^* / x_1 = I_1 a^* / x_2 \} x_3 \} \quad (2-28)$$

from which the resistance coefficient R_{11} can be defined from the ratio of voltage and total current, Φ_1/I_1 , as

$$R_{11} = x_1 / (r_{11} x_2 \} x_3 \} \quad (2-29)$$

For small changes of resistivity due to the deformation history, the previous expression for r_{11} can be expanded in an inverse series to give an approximation for R_{11} in the deformed configuration as

$$R_{11} = \frac{x_1 R_0}{x_2 \} x_3 \} (1 + R_{Y|Y} \underline{Y}| \underline{Y}| + R_{Y|Y} \underline{Y}| \underline{Y}| + R_{Y|Y} \underline{Y}| \underline{Y}| + R_{Y|Y} \underline{Y}| \underline{Y}|) + R_0 \dot{\underline{D}}$$

$$+ R_{Y|Y} \underline{Y}| \underline{Y}| + R_{Y|Y} \underline{Y}| \underline{Y}| + R_{Y|Y} \underline{Y}| \underline{Y}| \quad (2-30)$$

$$+ R_{Y|D} \underline{Y}| \dot{\underline{D}} + R_{Y|D} \underline{Y}| \dot{\underline{D}} + R_{DD} \dot{\underline{D}} \dot{\underline{D}}$$

where from the expansion and equations (2-22) the terms are

$$R_o = 1/r_{110} = 1/N_o c_{o11} \quad (2-31a)$$

$$R_{\gamma|} = (-N_o \Delta_{\gamma|} c_{11} - c_{o11} \Delta_{\gamma|} N)/R_o \quad (2-31b)$$

$$R_{\gamma]} = (-N_o \Delta_{\gamma]} c_{11} - c_{o11} \Delta_{\gamma]} N)/R_o \quad (2-31c)$$

$$R_o = (-N_o \Delta_{\alpha} c_{11} + c_{o11} \Delta_{\alpha} N) \Delta_D \alpha / R_o \quad (2-31d)$$

$$R_{\gamma| \gamma|} = -\Delta_{\gamma|} N \Delta_{\gamma|} c_{11} / R_o \quad (2-31e)$$

$$R_{\gamma| \gamma]} = (-\Delta_{\gamma|} N \Delta_{\gamma|} c_{11} - \Delta_{\gamma|} N \Delta_{\gamma]} c_{11}) / R_o \quad (2-31f)$$

$$R_{\gamma]} \gamma]} = -\Delta_{\gamma]} N \Delta_{\gamma]} c_{11} / R_o \quad (2-31g)$$

$$R_{\gamma| D} = -(\Delta_{\gamma|} N \Delta_{\alpha} c_{11} + \Delta_{\alpha} N \Delta_{\gamma|} c_{11}) \Delta_D \alpha / R_o \quad (2-31h)$$

$$R_{\gamma]} D} = -(\Delta_{\gamma]} N \Delta_{\alpha} c_{11} + \Delta_{\alpha} N \Delta_{\gamma]} c_{11}) \Delta_D \alpha / R_o \quad (2-31i)$$

$$R_{DD} = -\Delta_{\alpha} N \Delta_{\alpha} c_{11} \Delta_D \alpha \Delta_D \alpha / R_o \quad (2-31j)$$

The definitions given in equations (2-31) are the intrinsic resistance effects on electron density and transport from deformations. The coefficient term in equation (2-30) identifies the geometry-dependent resistance effects from deformations. This deformation-dependent coefficient can be rewritten for the case of spatially uniform strains and edge dislocation kinetics by using the following approximate relationships for the deformed length, width, and thickness dimensions of the test specimen in terms of the initial length $x_1|$, width $x_2|$, and thickness $x_3|$;

$$\begin{aligned} x_1| &= x_1| + u_1| + u_1] \\ &= x_1| (1 + \gamma_{11}| + \gamma_{11}]) \\ &= x_1| (1 + \gamma_{11}| + \int_0^t \dot{\Lambda}_{11}^D + \Lambda_{11}^{\dot{D}} dt) \end{aligned} \quad (2-32a)$$

$$x_2\} = x_2\} + u_2\} + u_2\} \quad (2-32b)$$

$$\doteq x_2\} (1 + \gamma_{22}\} + \int_0^t \dot{\Lambda}_{22}\} D + \Lambda_{22}\} \dot{D} \, d\tau)$$

$$x_3\} = x_3\} + u_3\} + u_3\} \quad (2-32c)$$

$$\doteq x_3\} (1 + \gamma_{33}\} + \int_0^t \dot{\Lambda}_{33}\} D + \Lambda_{33}\} \dot{D} \, d\tau)$$

Using the results from equations (3-32), the deformation dependent coefficient can be approximated by

$$\frac{x_1\}}{x_2\}x_3\} \doteq \frac{x_1\}}{x_2\}x_3\} (1 + \gamma_{11}\} + \int_0^t \dot{\Lambda}_{11}\} D + \Lambda_{11}\} \dot{D} \, d\tau)(1 - \gamma_{22}\} - \int_0^t \dot{\Lambda}_{22}\} D + \Lambda_{22}\} \dot{D} \, d\tau)(1 - \gamma_{33}\} - \int_0^t \dot{\Lambda}_{33}\} D + \Lambda_{33}\} \dot{D} \, d\tau) \quad (2-33)$$

Equation (2-33) can be further reduced by retaining only the first order terms and their associated cross-product terms to give a pure geometrical dependence of the deformations on a foil's resistivity;

$$\begin{aligned} \frac{x_1\}}{x_2\}x_3\} &= \frac{x_1\}}{x_2\}x_3\} (1 + \gamma_{11}\} - \gamma_{22}\} - \gamma_{33}\} \\ &+ \int_0^t (\dot{\Lambda}_{11}\} - \dot{\Lambda}_{22}\} - \dot{\Lambda}_{33}\}) D + (\Lambda_{11}\} - \Lambda_{22}\} - \Lambda_{33}\}) \dot{D} \, d\tau \\ &- \gamma_{11}\} \int_0^t (\dot{\Lambda}_{22}\} + \dot{\Lambda}_{33}\}) D + (\Lambda_{22}\} + \Lambda_{33}\}) \dot{D} \, d\tau \\ &- \gamma_{22}\} \int_0^t (\dot{\Lambda}_{11}\} - \dot{\Lambda}_{33}\}) D + (\Lambda_{11}\} - \Lambda_{33}\}) \dot{D} \, d\tau \\ &- \gamma_{33}\} \int_0^t (\dot{\Lambda}_{11}\} - \dot{\Lambda}_{22}\}) D + (\Lambda_{11}\} - \Lambda_{22}\}) \dot{D} \, d\tau \end{aligned} \quad (2-34)$$

This geometrical dependence can be substituted in equation (2-30); then retaining only first order terms and the first order cross-product terms, the expression for the (1-1) component of resistivity becomes

$$\begin{aligned} r_{11} = & \frac{x_1 |R_0}{x_2 |x_3|} (1 + G_{Y1} \underline{Y} | + G_{YJ} \underline{Y}] + G_{Y1YJ} \underline{Y} | \underline{Y}] \\ & + R_{Y1} \underline{Y} | + R_{YJ} \underline{Y}] + R_0 \bar{D} + (R_{Y1D} + G_{Y1} R_D) \underline{Y} | \bar{D} \\ & + (R_{YJD} + G_{YJ} R_D) \underline{Y}] \bar{D} + (G_{Y1} R_{YJ} + G_{YJ} R_{Y1} + R_{Y1YJ}) \underline{Y} | \underline{Y}] \end{aligned} \quad (2-35)$$

where the tensors G_{Y1} , G_{YJ} and G_{Y1YJ} are easily defined from the geometrical dependence given in equation (2-34) and squared strain terms $\underline{Y} | \underline{Y} |$ and $\underline{Y}] \underline{Y}]$ were omitted since only the cross-product terms were to be retained. The cross-product terms involving recoverable and nonrecoverable strains, $\underline{Y} | \underline{Y}]$, can be neglected in comparison to the other terms for most deformation histories because usually neither of these strains are large. The other term which will be neglected involves the product $\underline{Y}] \bar{D}$, primarily because this is a squared term in dislocation density effects. After removing these terms, the resistivity expression (2-35) reduces to

$$\begin{aligned} R_{11} = & \frac{x_1 |R_0}{x_2 |x_3|} (1 + G_{Y1} \underline{Y} | + G_{YJ} \underline{Y}] + R_{Y1} \underline{Y} | + R_{YJ} \underline{Y}] \\ & + R_D \bar{D} + (R_{Y1D} + G_{Y1} R_D) \underline{Y} | \bar{D} \end{aligned} \quad (2-36)$$

and contains a deformation dependence on the recoverable strain tensor $\underline{Y} |$, the nonrecoverable strain tensor $\underline{Y}]$, and dislocation density kinetics \bar{D} . The resistivity expression (2-36) has geometrical coefficients G_{Y1} and G_{YJ} to account for the recoverable and nonrecoverable dimensional changes of a resistor that change the total resistance. The intrinsic resistivity of the material has coefficients R_{Y1} , R_{YJ} , and R_D to account for linear interatomic dimensional effects from recoverable and dislocation dependent deformations. Finally, two cross-coupling effects from the coefficients R_{Y1D} and $G_{Y1} R_D$ are retained and describe a coupling between the recoverable strain and the dislocation kinetics.

The expression (2-36) for resistivity dependence on deformations is more general than previous elastic stress model given by Bridgeman [12] and the elastic stress plus plastic strain model developed by Chen, Gupta, and Miles [23] because of the explicit dependence on dislocation density and the cross-coupling terms. The explicit dependence of resistivity on dislocation density is more physically representative of mechanisms that cause changes in resistance; however, during an experiment the dislocation density is not an easily measured function throughout a deformation history. Nonetheless, terms involving the dislocation density could be evaluated with high voltage electron microscopy from experimental data for an improved representation of the elastic-plastic resistivity response.

III. Inference of Stress From Resistivity Changes

The resistivity expression (2-36) of the previous section depends on strain and dislocation density changes. The strain and dislocation density are appropriate physical variables that relate resistivity to atomic and scattering mechanisms of electron flux. If the recoverable strain tensor measure is elastic, then it can be uniquely replaced with a stress tensor dependence by using the elastic stress-strain relationship. However, if the nonlinear terms are retained in the approximate nonrecoverable strain tensor of equation (2-8), then resistivity would still depend on the recoverable strain tensor in a coupled and complex way. For small recoverable strain applications, these cross terms in the "plastic" strain could be neglected, and the classical assumption of plasticity that "elastic" and "plastic" strains are additive would result. This does not, however, imply that this resistivity model is based on the concepts of continuum mechanics because the representation of the nonrecoverable deformation and strains remains as a functional that depends on the dislocation density. Furthermore, the dislocation density is the source of the rate dependence in the resistivity response even though the recoverable strains are elastic. Thus, it is clear that the general resistivity model of equation (2-36) is complex and difficult to uncouple so that available experimental data on resistivity could be correlated with it. This model can be greatly simplified by the following assumptions:

A3.1 Assume that the recoverable strains are elastic.

A3.2 Assume that the nonlinear, or second order terms in the recoverable and nonrecoverable strains are small relative to the first order terms.

A3.3 Assume that the resistivity response depends only on the strains in the length, width, and thickness directions.

A3.4 Assume that the resistivity response of the material is isotropic.

A3.5 Assume that the elasticity response of the material is isotropic.

Based on the above assumptions, the second order tensors $\underline{\gamma}$ and $\underline{\gamma}$ have only a resistivity dependence from the three nonzero diagonal components 11, 22, and 33 when given in a coordinate frame with axes oriented such that x_1 is along the length direction, x_2 is along the width direction, and x_3 is along the thickness direction. Thus, the fourth order elastic-resistivity tensors of equation (2-36) do not depend on shear components and can be reduced to three-by-three matrices with components defined by diagonal and off-diagonal parameters as follows

$$R_{\underline{\gamma}} \equiv \begin{bmatrix} R_d & R_o & R_o \\ R_o & R_d & R_o \\ R_o & R_o & R_d \end{bmatrix} \quad (3-1a)$$

$$R_{\underline{\gamma}} \equiv \begin{bmatrix} R_d & R_o & R_o \\ R_o & R_d & R_o \\ R_o & R_o & R_d \end{bmatrix} \quad (3-1b)$$

$$\underline{R}_{\gamma} \text{]D} \equiv \begin{bmatrix} R_{\text{d}}^* \text{] } & R_{\text{o}}^* \text{] } & R_{\text{o}}^* \text{] } \\ R_{\text{o}}^* \text{] } & R_{\text{d}}^* \text{] } & R_{\text{o}}^* \text{] } \\ R_{\text{o}}^* \text{] } & R_{\text{o}}^* \text{] } & R_{\text{d}}^* \text{] } \end{bmatrix} \quad (3-1c)$$

The geometrical tensors $\underline{G}_{\gamma \text{]}}$ and \underline{G}_{γ} can also be now written as three-by-three matrices, which from equation (2-34) are seen to be equal to each other and given by

$$\underline{G}_{\gamma \text{]}} = \underline{G}_{\gamma} = \begin{bmatrix} 1 & 0 & 0 \\ 0 & -1 & 0 \\ 0 & 0 & -1 \end{bmatrix} \quad (3-2)$$

Then, the coupled geometrical-resistance tensor $\underline{G}_{\gamma \text{]}} R_{\text{D}}$ is given in matrix form as

$$\underline{G}_{\gamma \text{]}} R_{\text{D}} = \begin{bmatrix} R_{\text{D}} & 0 & 0 \\ 0 & -R_{\text{D}} & 0 \\ 0 & 0 & -R_{\text{D}} \end{bmatrix} \quad (3-3)$$

From equations (3-1) through (3-3), it is seen that this isotropic, elastic-plastic, shear-independent resistivity model has four scalar parameters and three functional operators to describe the intrinsic strain dependent resistance response of a material; namely, $R_{\text{d}} \text{]}$, $R_{\text{o}} \text{]}$, $R_{\text{d}} \text{]$, $R_{\text{o}} \text{]$, $R_{\text{d}}^* \text{]}$, and $R_{\text{o}}^* \text{]}$; and a functional operator R_{D} . Here, the intrinsic resistivity response that depends on the recoverable strain, through parameters $R_{\text{d}} \text{]}$ and $R_{\text{o}} \text{]}$ of tensor $R_{\gamma \text{]}}$ is defined as the "idealized" resistivity response of a material. For this intrinsic model, idealized resistivity is independent of the geometrical dimensional effects and of the dislocation density effects that change the resistance of a material test specimen.

Finally, using equations (3-1) through (3-3), equation (2-36) for the R_{11} component is written as

$$\begin{aligned}
 R_{11} = & \frac{R_0 X_1}{X_2 X_3} (1 + (\gamma_{11}^I - \gamma_{22}^I - \gamma_{33}^I) + (\gamma_{11}^J - \gamma_{22}^J - \gamma_{33}^J)) \\
 & + R_d |\gamma_{11}^I| + R_0^I (\gamma_{22}^I + \gamma_{33}^I) + R_d^J |\gamma_{11}^J| + R_0^J (\gamma_{22}^J + \gamma_{33}^J) \quad (3-4) \\
 & + R_D \dot{\bar{D}} + ((R_d^* + R_D) \gamma_{11}^I + (R_0^* - R_D) (\gamma_{22}^I + \gamma_{33}^I) \dot{\bar{D}})
 \end{aligned}$$

The resistivity expression (3-4) for the R_{11} component of an isotropic, thin rectangular foil can account for recoverable (elastic) and nonrecoverable (plastic) strain effects, dislocation density change effects, and cross-coupling between recoverable strains and dislocation density changes. It is only the R_{11} component from a tensor relationship for resistivity effects. The nonrecoverable (plastic) strain measures depend on dislocation transport and dislocation density changes that are described by first order terms in equations (2-8) and the approximation of equation (2-9).

The resistivity expression (3-4) extends the previous elastic-plastic resistivity model developed by Chen, Gupta, and Miles [23] because of the tensor aspects for nonrecoverable strain effects, the explicit rate dependence on dislocation density, and the cross-coupling term. The explicit rate dependence on dislocation density and the cross-coupling term are important in cases where nonrecoverable deformations have occurred. Such cases can arise when residual stress is to be inferred from the measured resistance change of a gage. Finally, the experimental data obtained by Chen, Gupta, and Miles [23] can be used to evaluate parameters of this extended model. This would include an evaluation of cross-coupling terms R_d^* , R_0^* and R_D to represent changes in the resistivity-strain slope that occurs for ytterbium and manganin materials during unloading from a plastic straining state. In Figures 3-1 and 3-2 experimental data from Chen, Gupta, and Miles [23] are shown of the resistance response versus a uniaxial elastic-plastic-unloading-reloading strain history for ytterbium and manganin. Without the cross-coupling terms in the model of equation (3-4), the elastic loading and unloading resistivity-strain slopes would be the same value. This extension of resistivity response could lead to improved gage designs that can respond to both elastic and plastic deformation histories, and still have an interpretable stress output.

Presently, the gage designs for deformation histories and subsequent inference of stress, particularly for ytterbium, are restricted to elastic responses. In the following discussion for just elastic response, this means that the terms of expression (3-4) involving γ_{11} , γ_{22} , γ_{33} , and $\bar{\theta}$ can be omitted as no dislocation density effects would occur during purely elastic material response. Then, equation (3-4) reduces to

$$R_{11} = \frac{R_0 X_1}{X_2 X_3} (1 + (\gamma_{11}) - \gamma_{22} - \gamma_{33}) + R_d |\gamma_{11}| + R_0 (\gamma_{22} + \gamma_{33}) \quad (3-5)$$

where the elastic-resistivity coefficients are R_d and R_0 . From assumption A3.5 the material is taken as isotropic and elastic, so equation (3-5) can be written in terms of stress as

$$R_{11} = \frac{R_0 X_1}{X_2 X_3} (1 + (1 + 2\nu) \sigma_{11} - \sigma_{22} - \sigma_{33})/E + (1 + \nu)(R_d - R_0) \sigma_{11}/E + ((1 - \nu) R_0 - \nu R_d)(\sigma_{11} + \sigma_{22} + \sigma_{33})/E \quad (3-6)$$

where the isotropic elasticity relationships for the diagonal strain components are

$$\begin{aligned} \gamma_{11} &= ((1 + \nu) \sigma_{11} - \nu (\sigma_{11} + \sigma_{22} + \sigma_{33}))/E \\ \gamma_{22} &= ((1 + \nu) \sigma_{22} - \nu (\sigma_{11} + \sigma_{22} + \sigma_{33}))/E \\ \gamma_{33} &= ((1 + \nu) \sigma_{33} - \nu (\sigma_{11} + \sigma_{22} + \sigma_{33}))/E \end{aligned} \quad (3-7)$$

and where ν and E are Poisson's ratio and Young's modulus, respectively. In terms of the notation used by Chen, Gupta, and Miles [23], their piezoresistance coefficients α and β are related to the intrinsic strain-resistivity coefficients, R_d and R_0 , by

$$\alpha = ((1 - \nu) R_0 - \nu R_d)/E \quad (3-8a)$$

$$\beta = (1 + \nu) (R_d - R_0)/2E \quad (3-8b)$$

Inverting equation (3-8), the elastic strain-resistivity coefficients in terms of the piezoresistivity coefficients α and β are

$$R_d | = (\alpha + 2\beta(1+\nu)/(1 + \nu)) E/(1 - 2\nu) \quad (3-9a)$$

$$R_o | = (\alpha + 2\beta\nu/(1 + \nu)) E/(1 - 2\nu) \quad (3-9b)$$

Using the experimental data measured by Chen, Gupta, and Miles [23] for ytterbium,

$$\nu = 0.365$$

$$E = 120 \text{ kb} \quad (3-10)$$

$$\alpha = - 0.788 \times 10^{-2}/\text{kb}$$

$$\beta = - 1.71 \times 10^{-2}/\text{kb}$$

dimensionless values of $R_d |$ and $R_o |$ for ytterbium from equation (3-9) are

$$R_d | = - 10.57 \quad (3-11)$$

$$R_o | = - 7.57$$

From an inspection of equation (3-5) or (3-6) the elastic dependent resistivity response of a foil is determined by knowing either the three independent components of strain, ($\gamma_{11} |$, $\gamma_{22} |$, $\gamma_{33} |$) or the three independent components of stress, (σ_{11} , σ_{22} , σ_{33}). Thus, a foil gage that is "ideally" embedded in a material would, by definition of ideally, sense the three independent components of strain, or equivalently, the three independent components of stress. For a constant current through the gage, the measured response from the gage would be the voltage, which from equation (2-28) is directly proportional to the resistance response of the foil. Clearly, a single resistivity history measurement for R_{11} cannot be used to determine uniquely the associated histories of three independent strain components or three independent stress components. This is because the resistivity change could be caused by a single component of strain or stress, or by a linear combination of the components. Thus, without special gage design to isolate and/or separate the effects of the different strain or stress components, or some special prior knowledge about two of the three components, it is not possible to infer multi-component strain or stress response from even an ideally embedded gage package.

There are at least two alternative approaches. The first was mentioned previously and consists of gage design such that single components of strain and stress are isolated and separated and then sensed by the resistance material; this is a standard current approach in piezoresistance gage development [30-36]. A second approach is suggested from the above discussed inability of a single gage to uniquely infer the multi-component state of strain or stress. Because there are only three independent components of either strain or stress that cause the resistivity response of most materials, it is conceptually possible to consider three "resistivity-independent" materials and to design a triple material gage package that provides three separate and simultaneous measurements of resistivity responses.

For purposes of illustration, consider three different materials labeled a, b, and c; and with elastic intrinsic strain-resistivity coefficients denoted by $R_d^a, R_o^a; R_d^b, R_o^b$; and R_d^c, R_o^c ; respectively. An illustration of a parallel configuration for a triple material gage package is shown in Figures 3-3. For this configuration, using equation (3-5) and assuming that the three materials are subjected to the same strain history, there are three separate and simultaneous resistivity responses from a triple material gage package given by

$$R_{11}^a = \frac{R_o^a X_1^a}{X_2^a X_3^a} (1 + (R_d^a + 1) \gamma_{11}) + (R_o^a - 1)(\gamma_{22} + \gamma_{33}) \quad (3-12a)$$

$$R_{11}^b = \frac{R_o^b X_1^b}{X_2^b X_3^b} (1 + (R_d^b + 1) \gamma_{11}) + (R_o^b - 1)(\gamma_{22} + \gamma_{33}) \quad (3-12b)$$

$$R_{11}^c = \frac{R_o^c X_1^c}{X_2^c X_3^c} (1 + (R_d^c + 1) \gamma_{11}) + (R_o^c - 1)(\gamma_{22} + \gamma_{33}) \quad (3-12a)$$

For three materials that are "resistivity-independent" means, by definition, that the above three equations can be inverted to determine the strain histories γ_{11}^I , γ_{22}^I , and γ_{33}^I . This is, of course, the strain history inferred for the three gages; and must be related to the strain history of the surroundings. In an "ideally strain embedded" gage package, the two would be identical. To illustrate the "ideally strain embedded" case for the three materials, equations (3-12) can be inverted to obtain the strains in terms of the three resistivity changes:

$$\begin{bmatrix} \gamma_{11}^I \\ \gamma_{22}^I \\ \gamma_{33}^I \end{bmatrix} = \begin{bmatrix} \gamma_{R1a} & \gamma_{R2a} & \gamma_{R3c} \\ \gamma_{R2a} & \gamma_{R2b} & \gamma_{R3c} \\ \gamma_{R3a} & \gamma_{R3b} & \gamma_{R3c} \end{bmatrix} \begin{bmatrix} \Delta R_a \\ \Delta R_b \\ \Delta R_c \end{bmatrix} \quad (3-13)$$

where the terms of the vector and matrix of equation (3-13) are given by

$$\begin{aligned} \Delta R_a &= (R_{11}^a - R_0^a x_1^a/x_2^a | x_3^a |) / (R_0^a x_1^a/x_2^a | x_3^a |) \\ \Delta R_b &= (R_{11}^b - R_0^b x_1^b/x_2^b | x_3^b |) / (R_0^b x_1^b/x_2^b | x_3^b |) \\ \Delta R_c &= (R_{11}^c - R_0^c x_1^c/x_2^c | x_3^c |) / (R_0^c x_1^c/x_2^c | x_3^c |) \\ \gamma_{R1a} &= ((R_d^b | + 1) (R_d^c | + 1) - (R_d^c | - 1)(R_d^b | - 1)) / \det \\ \gamma_{R2b} &= ((R_d^a | + 1) (R_d^c | + 1) - (R_d^c | - 1)(R_d^a | - 1)) / \det \\ \gamma_{R3c} &= ((R_d^a | + 1) (R_d^b | + 1) - (R_d^b | - 1)(R_d^a | - 1)) / \det \\ \gamma_{R1b} &= - ((R_d^c | + 1)(R_0^a | - 1) - (R_0^c | - 1)(R_0^a | - 1)) / \det \\ \gamma_{R1c} &= - ((R_d^b | + 1)(R_0^a | - 1) - (R_0^b | - 1)(R_0^a | - 1)) / \det \\ \gamma_{R2a} &= - ((R_d^c | + 1)(R_0^b | - 1) - (R_0^c | - 1)(R_0^b | - 1)) / \det \end{aligned} \quad (3-15)$$

$$\gamma_{R2c} = - ((R_d^a + 1)(R_o^b - 1) - (R_o^b - 1)(R_o^a - 1))/\det$$

$$\gamma_{R3a} = - ((R_d^b + 1)(R_o^c - 1) - (R_o^b - 1)(R_o^c - 1))/\det$$

$$\gamma_{R3b} = - ((R_d^a + 1)(R_o^c - 1) - (R_o^a - 1)(R_o^c - 1))/\det$$

and where the determinant det is given by

$$\begin{aligned} \det \equiv & (R_d^a + 1) ((R_d^b + 1) (R_o^c + 1) - (R_o^b - 1) (R_o^c - 1)) \\ & + (R_d^b + 1) ((R_d^a + 1) (R_o^c + 1) - (R_o^a - 1) (R_o^c - 1)) \\ & + (R_o^c + 1) ((R_d^a + 1) (R_d^b + 1) - (R_o^a - 1) (R_o^b - 1)) \end{aligned} \quad (3-16)$$

The above analysis demonstrates the conceptual basis for a triple material gage package from which the three diagonal components of strain can be computed. The condition of "resistivity-independent" materials is now placed in the context that the determinant defined by equation (3-16) cannot be zero; otherwise the inverse of equations (3-12) cannot be calculated. A non-zero determinant is a physical requirement that restricts the possible choice of materials for the gages; and it is of interest to check if any choice is available.

The experimental data of Chen, Gupta, and Miles [23], mentioned previously for ytterbium in equation (3-10), also reported values for manganin and constantan. The values reported for manganin were [23]

$$\begin{aligned} \nu &= 0.374 \\ E &= 876 \text{ kb} \\ \alpha &= -0.44 \times 10^{-3}/\text{kb} \\ \beta &= -0.31 \times 10^{-3}/\text{kb} \end{aligned} \quad (3-17)$$

and the values reported for constantan were [23]

$$\begin{aligned} \nu &= 0.33 \\ E &= 1461 \text{ kb} \\ \alpha &= -0.49 \times 10^{-4}/\text{kb} \\ \beta &= 1.64 \times 10^{-4}/\text{kb} \end{aligned} \quad (3-18)$$

Denoting the constantan as material "a", and using equation (3-9) and values from equation (3-18), the strain-resistivity coefficients are

$$\begin{aligned} R_{d}^a &= .51 \\ R_{o}^a &= .14 \end{aligned} \tag{3-19}$$

Denoting manganin as material "b", and using equation (3-9) and values from equation (3-17), the strain-resistivity coefficients are

$$\begin{aligned} R_{d}^b &= -2.51 \\ R_{o}^b &= -2.12 \end{aligned} \tag{3-20}$$

This leaves the ytterbium to denote as material "c", and from equation (3-11) its strain-resistivity coefficients are

$$\begin{aligned} R_{d}^c &= -10.57 \\ R_{o}^c &= -7.56 \end{aligned} \tag{3-21}$$

Using the values from equations (3-19) through (3-21), the determinant expression (3-16) can be evaluated to give

$$\det = + 61.87 \tag{3-22}$$

This shows that three "resistivity-independent" materials, namely constantan, manganin, and ytterbium, are available for a triple material gage.

The above analysis for a triple material gage demonstrates that three resistivity measurements can provide a unique determination of three diagonal components of strain. The three strain components are for an "ideally embedded" gage, and therefore, would be the strains of the gage material. By assuming an "ideally strain embedded" gage, we have assumed that these are the strains of the surrounding material. In practical applications, there would exist a mismatch of material properties between the surrounding material and the gage materials; hence, "ideal strain embedding" would not be physically possible, but may be a reasonable approximation for some applications. However, in other practical applications, further analysis would be required

because strain tensor continuity across a boundary interface between two different materials is not always satisfied. The problem of stress and/or strain continuity conditions has been discussed previously by Gupta [22]. For elastic response and perfect bonding, the condition of normal stress continuity at a material interface is an equilibrium condition. The tangential conditions on stress components at a material interface, however, can be discontinuous. For perfect bonding of the materials at a planar interface, the tangential strain components are continuous across the interface boundary. Thus, the boundary interface between the resistivity materials and the surrounding material must be represented in order to make an inference of strain-stress response of the surrounding material. In this case, a hybrid gage analysis involving both the stress and the strain resistivity responses for the three materials of the gage is required for one to infer the stress-strain response of the surrounding material.

For thin gages placed normal to the shock front, a hybrid stress-strain coupling between the gage surfaces and the surrounding material is a reasonable and practical approximation in that the time interval for stress ring-up in the thickness direction is small. In this case, the thickness coordinate is the x_3 direction; therefore, the σ_{33} stress component is required to be continuous between the gage and surrounding material. The tangential directions of the gage are the length and width dimensions along the x_1 and x_2 coordinates, so the strain coupled portion of the resistivity response of AR_{11} is due to γ_{11} and γ_{22} components of the strain tensor. For a thin gage that is bonded to the surrounding material, it follows that the displacement across the gage-material interface is continuous; hence, the γ_{11} and γ_{22} strain components in the gage and in the adjacent surrounding material are equal. Equations to represent this combination of stress and strain dependent resistivity for the elastic gage response are obtained by first expressing the σ_{33} stress component in equations (3-7) as a function of strain; thus

$$\sigma_{33} = (\gamma_{33}) + \nu(\gamma_{11} + \gamma_{22}) + \gamma_{33}/(1-2\nu)E/(1+\nu) \quad (3-23)$$

$$\gamma_{33}| = ((1+\nu)(1-2\nu)\sigma_{33}/E - \nu(\gamma_{11}| + \gamma_{22}|))/(1-\nu) \quad (3-24)$$

Finally, $\gamma_{33}|$ of equation (3-24) is substituted into equation (3-5) to obtain an expression of the elastic resistivity response for a gage oriented normal to the x_3 coordinate in terms of the normal stress σ_{33} and the tangential strain components $\gamma_{11}|$ and $\gamma_{22}|$ in the gage; namely,

$$\begin{aligned} R_{11} = \frac{R_0 X_1 |}{X_2 | X_3 |} & (1 + (1 + (1-\nu)R_d| - \nu R_0)|\gamma_{11}|/(1-\nu) \\ & + (1-2\nu)(R_0| - 1)\gamma_{22}|/(1-\nu) \\ & + (1-2\nu)(1+\nu)(R_0| - 1)\sigma_{33}/(E(1-\nu))) \end{aligned} \quad (3-25)$$

In the above expression, R_{11} resistivity depends on the strain components $\gamma_{11}|$ and $\gamma_{22}|$, and the stress component σ_{33} ; thus, it would again require three independent resistivity gages before the strains $\gamma_{11}|$, $\gamma_{22}|$, and the stress σ_{33} could be inferred. Conceptually, this is analogous to the three strain response of equation (3-13) for the three different materials and a detailed analysis is not repeated.

From the above analyses, whether an "ideally strain embedded" gage or for the case of a coupled stress and strain gage, it is certainly clear that a gage of a single material configuration is not sufficient to uniquely infer multi-stress or multi-strain history responses. Furthermore, it has been demonstrated that a triple material gage configuration is physically possible and that for an "ideally" embedded case one can uniquely determine multi-strain history responses of the gage material.

In practice, an embedded gage may not always respond as "ideally" assumed in the above discussion, and the gage becomes an "inclusion" problem [19,22]. The "inclusion" problem occurs when the embedded gage does influence the response of the surrounding material for which stress or strain is to be inferred. Conditions for "ideally" embedded gage responses are not well established, but depend on the material property parameters of the gage and surrounding materials and on the dimensions and bonding of the gage to the surrounding material. Small differences between material property parameters is desirable. When small differences are not the case, then it is known from the composite materials that the dimensions and bonding of the gage can significantly modify the local stress-strain fields of the surrounding material. An effective way of representing this modification is the shear-lag model developed for composite material response [41,42].

IV. Summary

Previous material models developed for the intrinsic resistivity change due to recoverable deformations have been related to the stress tensor; hence, the term piezoresistivity. However, the physical mechanisms associated with changes of electron transport, or resistivity, in an atomic lattice structure are more directly related to deformation measures and dislocation defect structures of the atomic lattice. Using the concepts of discontinuum mechanics which separates deformations into a recoverable function term and a nonrecoverable functional term, a model for the intrinsic resistivity response of a material was developed that had deformation measures of recoverable strain tensor, dislocation dependent nonrecoverable strain tensor, and dislocation density kinetics. In the simplest case, the recoverable strain is the elastic strain, the nonrecoverable strain tensor reduces to an explicit dislocation dependent plastic strain measures, and the dislocation density kinetics term represents changes in the atomic lattice to account for mobile electron density changes and electron-dislocation density cross-sectional scattering changes. Therefore, this model for intrinsic resistivity of a material relates physical aspects of electron band configurations and electron scattering in terms of interatomic deformation measures dislocation defect structures.

However, as discussed in Section II, the intrinsic resistivity of a material is only part of the resistivity response that is observed during a typical experimental configuration involving a deformation history of a material specimen. This is because the deformation history also changes the overall dimensions of the material specimen and results in a geometry dependence. For spatially uniform deformations, which means that the recoverable and nonrecoverable strains are uniform over the volume of the material specimen, the geometry dependence can be represented in terms of the strains.

Although non-uniformities in the initial dimensions of a material test specimen were not analyzed in this report, it is believed that experimental resistivity measurements on thin rectangular foils may have a high sensitivity to non-uniform variations of the initial dimensions. This is mentioned as it

could be one possible source of the differences in measured values for the elastic-resistivity coefficients often discussed in the literature [21,23,25,26].

The simplified elastic-plastic resistivity model of Section II generalizes a previous model developed by Chen, Gupta, and Miles [23]. The generalizations are due to the tensor dependence on the nonrecoverable (plastic) strain tensor and on an explicit dislocation dependent defect structure. Furthermore, a cross-coupling term between the recoverable strain and the dislocation dependent defect structure was retained in the simplified resistivity model so that the change in resistivity during an elastic unloading from a plastic straining history value could be represented. This type of generalization in the resistivity model is considered important for the design of gages to measure and interpret residual stress states after strong shock loading. At this time, however, further analysis is required to relate the experimental data [23] to this (elastic-dislocation resistivity) model. Such analysis is necessary to extend gage development into the elastic-plastic range of material and resistivity response; otherwise, the uncertainty of the interpretation of the stress measured will remain large.

The significant aspects that result from this development of a deformation dependent model of resistivity are discussed in Section III. This section describes in detail shear-independent intrinsic resistivity and the geometrical resistivity responses of isotropic, elastic materials in terms of strain and/or stress. This discussion leads to a conceptual design for a triple material gage package that measures three simultaneous and separate resistance changes as output. Under ideal strain embedding conditions of the gage and when the three materials of the gage are "resistivity-independent", then the gage output can be inverted to obtain the three independent diagonal components of the strain tensor. This is important because, in most experimental situations, measurement for multi-component values of the stress or strain tensor is of interest. A coupled stress-strain analysis of triple material gage response is described for cases where the ideal strain embedding assumption is relaxed. This involves using both the strain and stress dependent resistivity responses of the three materials contained in the gage, then, coupling the material surrounding the gage to the materials of the gage by a consistent set of displacement and stress continuity boundary conditions

at the various material interfaces. As discussed by Gupta [22], this analysis problem exists for all embedded gages; its resolution is the key to any inference of the stress state in the surrounding material. Even for what initially appears as one-dimensional cases without the embedded gage, the same problem with the embedded gage becomes non-trivial because a consistent set of interface boundary conditions in practical applications may suggest a significant degree of three-dimensional coupling between the gage and the surrounding material. This is probably most significant in low shear and tensile strength materials such as high porosity rock and alluvium. Certainly, when the initial case has a multi-component stress field that will interact with the embedded gage, an understanding of the gage response coupled to the surrounding material is required before the measured data can be interpreted and the stress inferred.

Acknowledgments

The author wishes to thank G. Anderson, D. Glenn, B. Hudson, J. Kalinowski, E. Kansa, D. Larson, and L. Thigpen for their willingness to share both literature and knowledge. Also, all of the information obtained from discussions and correspondence with B. Bass, A. Florence, Y. Gupta, D. Keough, D. Patch, and C. Smith is greatly appreciated. L. Grabowski is especially thanked for the excellent typing and organization of the paper.

The author wishes to thank the Nuclear Test Containment Program for supporting this work. Work performed under the auspices of the U.S. Department of Energy by the Lawrence Livermore National Laboratory under contract number W-7405-ENG-48.

References

1. Mason, W. P., Crystal Physics of Interaction Processes, Academic Press, NY, 1966, pp 221-240.
2. Madelung, O., Physics of III-V Compounds, John Wiley & Sons, NY, 1964, pp 180-185.
3. Solymer, L., and D. Walsh, Lectures on the Electrical Properties of Materials, Oxford University Press, Oxford, 1984, pp 121-148.
4. Kao, C. K., and Hwang, W., Electrical Transport in Solids, with Particular Reference to Organic Semiconductors, Pergamon Press, Oxford, 1981, pp 1-61.
5. Savelyev, I. V., Physics, A General Course, Mir Publishers, Moscow, 1981, pp 158-207.
6. Haug, A., Theoretical Solid State Physics, Vol. 2, Pergamon Press, Oxford, 1972, pp 1-52 and 142-193.
7. Ziman, J. M., Electrons and Phonons, the Theory of Transport Phenomena in Solids, Clarendon Press, Oxford, 1960, pp 174-447.
8. Herring, C., "Transport Properties of a Many-Valley Semiconductor," *Bell Syst. Tech. J.*, Vol. XXXIV, pp 237, 1955.
9. Brown, R. A., "Scattering Theory for Crystal Dislocations," *J. Phys. F: Metal. Phys.*, Vol. 7, pp 1269, 1977.
10. Brown, R. A., "Electrical Resistivity of Dislocations in Metals," *J. Phys. F: Metal Phys.*, Vol. 7, pp 1283, 1977.
11. J. Yamashita, "Volume Dependence of the Electrical Resistivity of Sodium," *J. Phys. F: Metal Phys.*, Vol. 12, pp 713, 1982.
12. Bridgman, P. W., "The Effect of Homogeneous Mechanical Stress on the Electrical Resistance of Crystals," *Phys. Rev.*, Vol. 42, pp 853, 1932.
13. Hollander, L. E., G. L. Vick, and T. J. Diesel, "The Piezoresistive Effect and Its Applications," *Rev. of Sci. Inst.*, Vol. 31, pp 323, 1960.
14. Keough, D. D., and J. Y. Wong, "Variation of the Shock Piezoresistance Coefficient of Manganin as a Function of Deformation," *J. Appl. Phys.*, Vol. 41, pp 3508, 1970.
15. Bareis, E., E. Williams, and C. Skoog, "Piezoresistivity Coefficients in Manganin," *J. Appl. Phys.*, Vol. 41, pp 5:55, 1970.
16. Lee, L. M., "Nonlinearity in the Piezoresistance Coefficient of Impact-loaded Manganin," *J. Appl. Phys.*, Vol. 44, pp 4017, 1973.

17. Ginsberg, M. J., D. E. Grady, P. S. DeCarli, and J. T. Rosenberg, "Effects of Stress on the Electrical Resistance of Ytterbium and Calibration of Ytterbium Stress Transducers," Stanford Research Institute report for contract DNA001-72-C-D146, DNA 3577F, August 1973.
18. Grady, D. E., and M. J. Ginsburg, "Piezoresistive Effects in Ytterbium Stress Transducers," J. Appl. Phys., Vol. 48, pp 2179, 1977.
19. Rosenberg, Z., D. Yaziv, and Y. Partom, "Calibration of Foil-like Manganin Gauges in Planar Shock Wave Experiments," J. Appl. Phys., Vol. 51, pp 3702, 1980.
20. Gupta, Y. M., D. D. Keough, D. Henley, and D. F. Walter, "Measurement of Lateral Compressive Stresses Under Shock Loading," Appl. Phys. Lett., Vol. 37, pp 395, 1980.
21. Gupta, Y. M., "Analysis of Manganin and Ytterbium Gauge Data Under Shock Loading," J. Appl. Phys., Vol. 54, pp 6094, 1983.
22. Gupta, Y. M., "Stress Measurements Using Piezoresistance Gauges: Modeling the Gauge as a Elastic-Plastic Inclusion," J. Appl. Phys., Vol. 54, pp 6256, 1983.
23. Chen, D. Y., Y. M. Gupta, and M. H. Miles, "Quasistatic Experiments to Determine Material Constants for the Piezoresistance Foils Used in Shock Wave Experiments," J. Appl. Phys., Vol. 55, pp 3984, 1984.
24. Gupta, S. C., and Y. M. Gupta, "Piezoresistance Response of Longitudinally and Laterally Oriented Ytterbium Foils Subjected to Impact and Quasi-static Loading," J. Appl. Phys., Vol. 57, pp 2464, 1985.
25. Rosenberg, Z., and Y. Partom, "Piezoresistance Gauges," J. Appl. Phys., Vol. 58, pp 1814, 1985.
26. Brar, N. S., and Y. M. Gupta, "Piezoresistance Response of Different Batches of Ytterbium Foils," pre-publication copy, December 1985.
27. Nagy, G., and A. L. Florence, "Laboratory Experiments on Spherical Waves in Geologic Materials," Third Symp. on Containment of Underground Nuclear Explosions, Vol. 1, pp 296, C. Olsen, Ed., Lawrence Livermore National Laboratory, September 1985.
28. Stout, R. B., and D. B. Larson, "Finite Deformations, Onsager Irreversible Thermodynamics, and Stress Wave Analysis of Shock Waves," Third Symp. on Containment of Underground Nuclear Explosions, Vol. 1, pp 314, C. Olsen, Ed., Lawrence Livermore National Laboratory, September 1985.
29. Larson, D. B., Stress Gauge Measurements in Spherical Diverging Flows, Third Symp. on Containment of Underground Nuclear Explosions, Vol. 1, pp 214, C. Olsen, Ed., Lawrence Livermore National Laboratory, September 1985.

30. Keough, D. D., "Procedure for Fabrication and Operation of Manganin Shock Pressure Gages," Stanford Research Institute report AFWL-TR-68-37 for contract AF29(601)-68-C-0038, August 1968.
31. Keough, D. D., "Development of a High-Sensitivity Piezoresistive Shock Transducer for the Low Kilobar Range," Stanford Research Institute report DSA 2508 for contract DASA 01-69-0014, March 1970.
32. Glenn, H. D., "Diagnostics Techniques Improvement Program; High Explosives Development Phase," Systems, Science and Software report DNA 29781, September 1972.
33. Glenn, H. D., "Development of Diagnostic Techniques for Application to Underground Nuclear Tests," Systems, Science, and Software report DNA 3257F, October 1973.
34. Smith, C. W., "PUFF TOO: A Residual Stress Experiment," Sandia National Laboratories report SAND 79-1674, April 1980.
35. Glenn, H. D., T. F. Stubbs, J. A. Kalinowski, and E. C. Woodward, "Containment Analysis for the Queso Nuclear Event," Proc. Second Symp. on Containment of Underground Nuclear Explosions, Vol. 1, pp 411, Kirtland AFB, Albuquerque, NM, C. Olsen, Ed., Lawrence Livermore National Laboratory, August 1983.
36. Smith, C. W., "ONETON: A High-Explosive Containment Experiment in Wet Tuff," Sandia National Laboratory report SAND 84-1073, October 1984.
37. Kalinowski, J., J. R. Hearst, B. C. Hudson, J. Charest, and L. Davies, Stress Measurement Development at LLNL, Third Symposium on Containment of Underground Nuclear Explosions, Vol. 3, pp 79, Idaho Falls, ID, C. Olsen, Ed., Lawrence Livermore National Laboratory, September 1985.
38. Stout, R. B., "Note on Strain Rate, Dislocation Density, Dislocation Motion, and Dislocation Constitutive Equations," Cryst. Latt. Def., Vol. 9, pp 47, 1980.
39. Stout, R. B., "Modelling the Deformations and Thermodynamics for Materials Involving A Dislocation Kinetics," Cryst. Latt. Def., Vol. 9, pp 65, 1981.
40. Stout, R. B., "A Model for the Deformations and Thermodynamics of Liquids Involving a Dislocation Kinetics," Rheologica Acta, Vol. 21, pp 659, 1982.
41. Hedgepeth, J. M., and P. VanDyke, "Local Stress Concentration in Imperfect Filamentary Composite Materials", J. Composite Mat., Vol. 1, pp 294, 1967.
42. Fukuda, H., and Chou, T., "An Advanced Shear-Lag Model Applicable to Discontinuous Fiber Composites", J. Composite Mat., Vol. 15, pp 79, 1981.

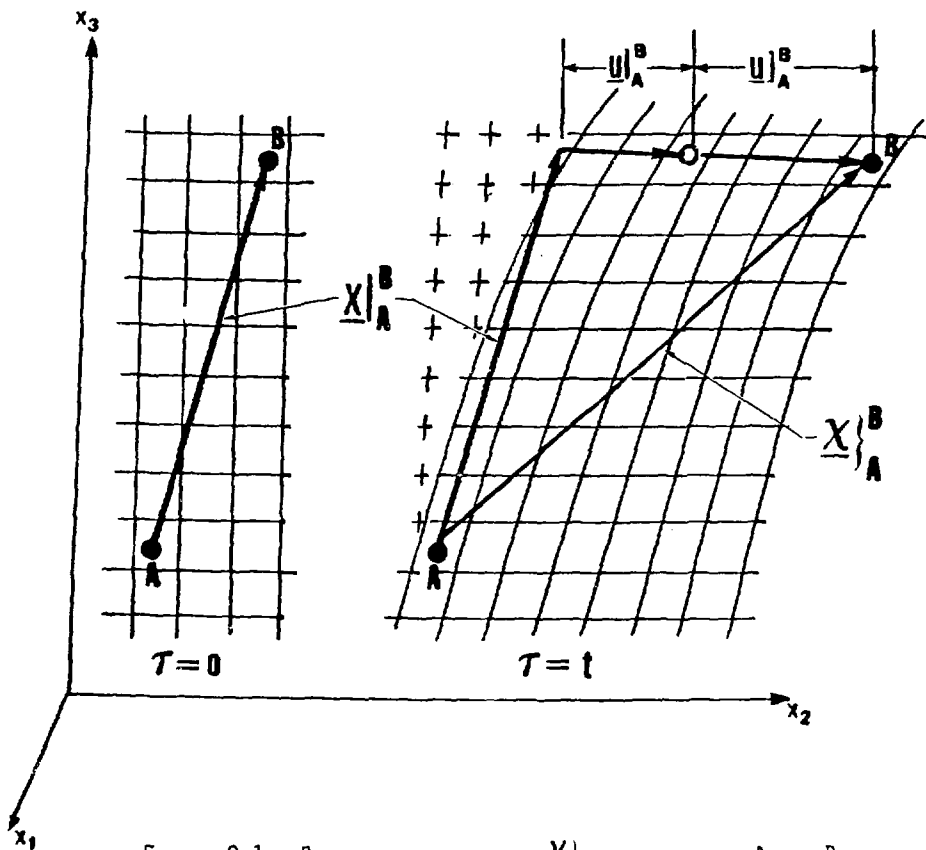


FIGURE 2-1. RELATIVE DEFORMATION X_A^B BETWEEN ATOMS A AND B FROM CONTINUOUS AND DISCONTINUOUS DISPLACEMENTS u_A^B AND u_A^B DURING TIME INTERVAL τ .

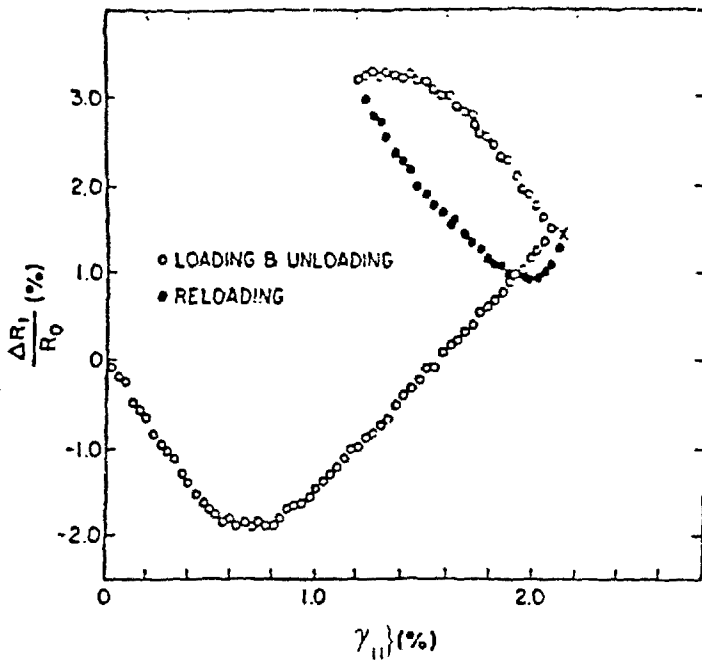


FIGURE 3-1. YTTERBIUM RESISTIVITY RESPONSE DURING UNIAXIAL ELASTIC-PLASTIC STRAIN HISTORY (REF. 23).

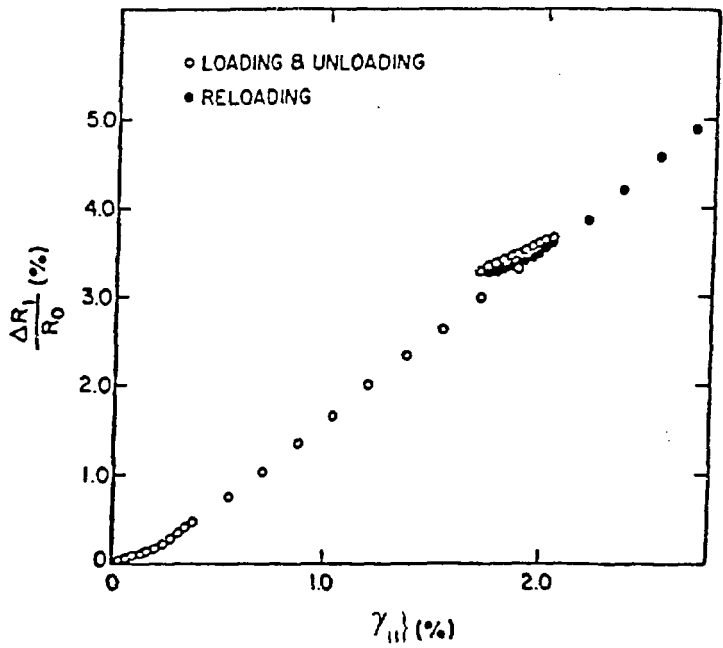


FIGURE 3-2. MANGANIN RESISTIVITY RESPONSE DURING UNIAXIAL ELASTIC-PLASTIC STRAIN HISTORY (REF. 23).

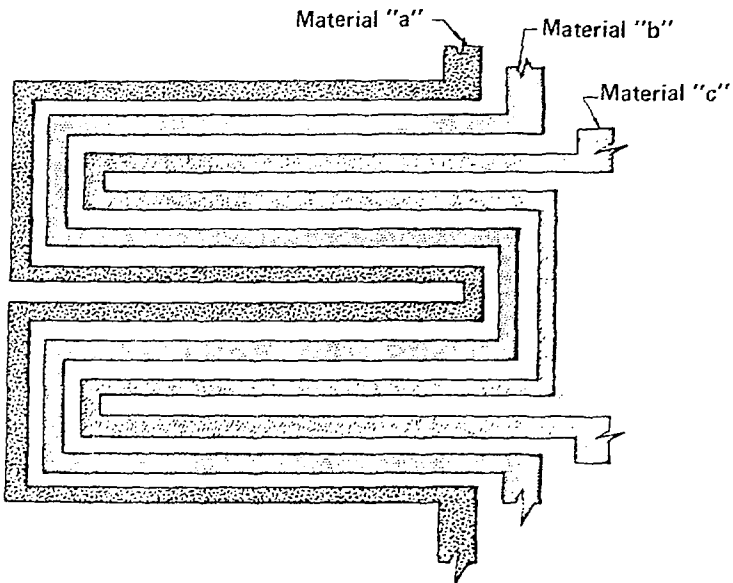


FIGURE 3-3. TRIPLE MATERIAL FOIL GAGE TO MEASURE THREE DIAGONAL COMPONENTS OF STRAIN OR STRESS COMPONENTS.